Hot Compaction of Polyoxymethylene, Part 1: Processing and Mechanical Evaluation

K. Al Jebawi,[1] B. Sixou,[1] R. Séguéla,[1]* G. Vigier,[1] C. Chervin[2]

[1]*Groupe d'Etudes de Métallurgie Physique et de Physique des Matériaux, INSA de Lyon, Batiment Blaise Pascal, 69621 Villeurbanne, France*
[2]*European Technical Center, Du Pont de Nemours, Le Grand, Saconnex, Geneva CH-1218, Switzerland*

Received 22 August 2005; accepted 24 January 2006
DOI 10.1002/app.24342
Published online in Wiley InterScience (www.interscience.wiley.com).

ABSTRACT: The hot-compaction of polyoxymethylene powders in the solid state, otherwise pressure-assisted sintering, is studied as an alternative way to the melt-compression or injection molding processes. A native powder issued from suspension polymerization has been used, together with powders obtained from grinding of melt-extruded pellets. The experimental conditions were optimized with regard to temperature, pressure, and time. Temperature is the most sensitive parameter of the process. Sintering at temperature close to the onset of the melting range turned out to be necessary for an efficient welding of the powder particles, as judged from mechanical properties. Despite a strong loss of ductility, the sintered samples have been easily machined out into strips for mechanical testing. A significant increase in crystallinity is observed for the sintered samples, as compared with the compression-molded ones, accompanied with a nearly twofold increase of the Young's modulus. Scanning electron microscopy revealed that rupture of the sintered samples involves both inter- and intra-granular fracture. Welding of the crystallites via molecular diffusion at the particle interface is suggested to be the mechanism of sintering. © 2006 Wiley Periodicals, Inc. J Appl Polym Sci 102: 1274–1284, 2006

Key words: polyoxymethylene; powders; compaction; sintering; mechanical behavior

INTRODUCTION

Powder sintering has been developed for processing high melting point materials, such as metallic alloys or ceramics, at temperatures far below their melting point, to reduce energy consumption and avoid difficulties connected with the manipulation of liquids at very high temperature. The basic mechanism of sintering is the diffusion of atoms at the powder grain boundaries after the powder has been compacted as close as possible to the so-called theoretical density. The reduction of porosity between grains during the compaction stage is a determining factor for the efficiency of the sintering process. A high specific surface is also beneficial for the welding of the powder grain.

Sintering is not currently used in the domain of polymeric materials. Nevertheless, it is an efficient means for processing amorphous polymers having high thermal stability[1,2] at temperatures far below that of melt-processing methods such as injection or extrusion. This technique helps to prevent thermal degradation. It is also a helpful means to incorporate mineral or metallic filers at larger amounts than allowed by melt processing.

Sintering of polymer powders also proved to be a solution for polymer processing when extrusion or injection are not allowed due to very high viscosity of materials having very high molar weight. This is typically the case of polytetrafluoroethylene (PTFE)[1–3] and ultra-high molar weight polyethylene (UHMWPE),[4,5] for which only few investigations have been yet reported. The processing of such polymer powders is usually carried out in two stages: compacting at room temperature (RT) followed by annealing at a temperature above the melting point, to achieve the welding of the powder grains. Regarding the terminology of powder metallurgy, this is not a true sintering process: as a matter of fact, the material looks like a solid due to its extremely high viscosity, but the welding of the powder grains actually occurs in a thermodynamically molten state.

Very few examples of true sintering of polymer powders have been reported in literature, notably regarding semicrystalline polymers. Statton[6] first reported the sintering of polyethylene single crystal mats during annealing below the melting point. The initially brittle mats turned highly ductile after long time annealing. The mechanism of the welding of the single crystals was ascribed to a mutual interdiffusion

**Present address:* Laboratoire "Structure et Propriétés de l'Etat Solide," Université de Lille1, Batiment C6, 59655 Villeneuve d'Ascq, France.

Correspondence to: R. Séguéla (roland.seguela@univ-lille1.fr) or G. Vigier (gerard.vigier@insa-lyon.fr).

of chains between neighboring crystals. More recently, Rastogi and coworkers[7,8] reported that UHMWPE native powders can be efficiently sintered under high pressure; thanks to the phase transition from the orthorhombic crystalline form to the high temperature hexagonal form, owing to the high molecular mobility of the latter crystalline form.

In the case of UHMWPE powders, it has been shown that a highly cohesive material can be obtained by applying a high level of plastic deformation below the melting point: this can be achieved by solid state extrusion of either solution-grown single crystal powders[9] or native reactor powders.[10,11] The final drawn films display an excellent cohesion in addition to a high longitudinal stiffness due to molecular orientation. The welding of the powder particles during the process seems to be highly improved by the shear strain. Similar to UHMWPE, single crystal mats and reactor powders of ultra-high-molar-weight polypropylene and poly(4-methyl-1-pentene) also displayed good processability by solid state extrusion.[12]

Ward and coworkers have extensively studied the static hot compaction of various kinds of synthetic polymer fibers, notably ultra-high modulus/ultra-high strength UHMWPE fibers[13–17] for manufacturing light monolithic composites with high impact properties. In the case of melt-spun fibers, the best performances are reached when compaction is carried out in the temperature window corresponding to the melting range of the material: the efficiency of the process has been ascribed to the partial melting of the fiber surface, followed by an epitaxial crystallization of the melted fraction of the fibers on the remaining non-melted part. The recrystallized part of the material builds up a strongly binding medium for the oriented fibers, preserving most of their initial strength and stiffness. In the case of gel-spun fibers, carrying out the compaction in the lower range of the temperature window enables a localized deformation-induced welding of the fibers[14] without significant surface melting and recrystallization.

Polyoxymethylene (POM) is a semicrystalline thermoplastic polymer with valuable mechanical properties such as high stiffness, hardness, fatigue, and creep resistance, in conjunction with low friction and wear resistance.[18] These properties make POM particularly suited for manufacturing fixture gears, fan, and pump propellers, bearing liners and rings, gear wheels and pinions, etc. POM is also currently used for prototyping owing to its excellent ability for machining. However, POM suffers from two main shortcomings: a significant shrinkage of injection-molded parts and a natural trend for thermal decomposition, namely depolymerization about the melting point. Sintering of POM powders below the melting point was then suspected to be a means to avoid the two previous drawbacks.

TABLE I
Physical Characteristics of the Materials

Material	W_c (wt %)	ϕ_c (vol %)	$T_{f\,\mathrm{peak}}$ (°C)	$T_{f\mathrm{onset}}$ (°C)
POM-N	87	—	177.0	170
POM-G	74	—	175.5	168
POM-NS	92	88	181.5	
POM-GS	86	82	181.5	
POM-CM	68	64	175.0	165
KEP-G	53	—	166.5	160
KEP-GS	60	—	169.0	
KEP-CM	53	—	166.0	160

W_c, crystal weight fraction; ϕ_c, crystal volume fraction; $T_{f\,\mathrm{peak}}$, temperature at melting peak; and $T_{f\,\mathrm{onset}}$, temperature of the melting onset.

Similar to POM, poly(aryl-ether-ether-ketone), otherwise PEEK, is a semicrystalline polymer highly sensitive to thermal degradation during melt-processing due to its high melting point close to 335°C. Sintering proved to be a means to prevent degradation and also to incorporate large amounts of metallic powder for producing conductive parts.[1,2] The main differences between the two materials is that the POM melting point is significantly lower than that of PEEK, and that the POM glass transition is far below RT while that of PEEK is far above. These thermal features should be responsible for great differences regarding the sintering mechanism of the two materials and the optimization of the process.

This article deals with the optimization of the sintering parameters under pressure of POM native reactor powders as well ground powders, below the melting point. Mechanical and thermal properties are used to evaluate the efficiency of the process. Comparisons are made with a sample prepared by compression-molding of the same POM material above the melting point. The sintering of a copolymer having lower crystal content than the homopolymer is also investigated.

MATERIALS AND EXPERIMENTAL METHODS

A native polyoxymethylene powder, POM-N, issued from suspension catalytic polymerization has been supplied by Du Pont, Switzerland. Its weight–average molar weight was M_w = 35 kDa. The crystal weight fraction, melting point at peak, and melting onset of the POM-N powder are reported in Table I. A powder cryogenically ground from pellets of melt-extruded POM-N has also been provided by Du Pont. The data in Table I show that this powder, named POM-G, has significantly lower crystalline perfection than the virgin powder as judged from the lower crystal content and the lower melting point.

A Kepital 320 copolymer from Korea Engineering Plastics has been investigated comparatively. Accord-

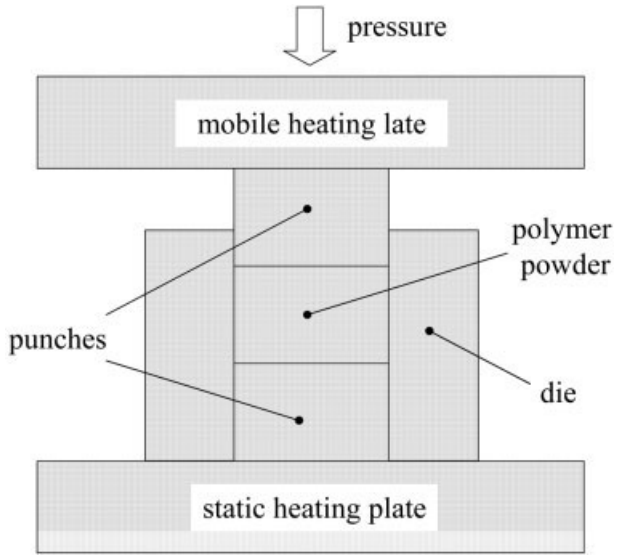

Figure 1 Sketch of the sintering device.

ing to literature data*, this copolymer contains about 2 mol % of randomly distributed ethylene-oxide units. A ground powder, named KEP-G, has been prepared by cryogenic grinding of the as-received pellets.

All the powders have been sieved prior to hot compacting to discard all particles and agglomerates larger than 200 μm.

The processing of powders into bulk pieces has been carried out by hot compaction under pressure in the solid state, i.e., below the melting point. The powder was introduced in the compression cell, which consists of a cylindrical die and two punches, as shown in Figure 1. The filled cell was then preheated in an oven at 110°C for 30 min, before being inserted between the plates of a heating press for the compacting operation. An insulating cloth was wrapped around the die to prevent convective heat dissipation. The optimization of the heating cycle together with the loading and unloading pathway of the experiment is described in the next section. For reasons of simplicity, the whole hot compacting operation, or pressure-assisted sintering, will be called "sintering process" throughout the article.

The sintered pieces were in the form of 10 mm thick discs of diameter 60 mm. The materials sintered from the native and ground POM powders were designated POM-NS and POM-SG, respectively. The material sintered from the Kepital ground powder is called KEP-GS. Samples for mechanical testing were machined out from the discs using a milling cutter. Figure 2 shows how the samples have been cut out from the original discs for carrying out the mechanical experiments.

For the sake of comparison with the sintered materials, compression-molded samples of both POM and KEP were also prepared. The powders or pellets were melted for 5 min between steel plates, at 220 and 210°C, for POM and KEP, respectively. The 10 mm thick compression-molded pieces, called POM-CM and KEP-CM, were cooled down to RT at about 20°C/min.

The physical characterization of the samples has been carried out by means of differential scanning calorimetry (DSC), on a Perkin–Elmer DCS7 apparatus. The heating curves were recorded at a scanning rate of 10°/min, using samples of about 6 mg. The crystal weight fraction, W_c, was determined from the melting enthalpy of the samples, assuming a melting enthalpy of 260 J/g for perfectly crystalline POM,[19] with an uncertainty of $\pm$30 J/g. The crystal volume fraction, ϕ_c, was computed from the crystal weight fraction using the following values ρ_c = 1.49 g/cm^3 and ρ_a = 1.21 g/cm^3 for the densities of the crystalline and amorphous components.[20] Apparent density determinations were also performed by pycnometry as well as by weight and volume measurements on the sintered discs.

To evaluate the efficiency of the sintering of the materials, three-point bending tests were achieved up to rupture, the breaking stress being taken as a measurement of the interparticle cohesion. Experiments were carried out on an Instron testing machine according to the ISO-178 Norm: the samples were 3 mm thick, 10 mm wide, and 56 mm long. The distance between the two external contacts was 50 mm, and the cross-head speed on the central contact was 100 μm/min. The reported data are averaged from three measurements. The stress scatter did not exceed 10% about the average values.

Compressive tests were carried out on the same Instron machine at a cross-head speed of 100 μm/min using 8 $\times$ 8 $\times$ 10 mm^3 parallelepiped samples. In that configuration, the machine compliance was not negligible and correction was applied on the strain measurements owing to the stress–strain recording from a steel sample of similar dimensions.

Dynamic mechanical analysis (DMA) has been conducted on an oscillation-forced torsion pendulum, as a function of temperature, at the frequency of 1 Hz. The

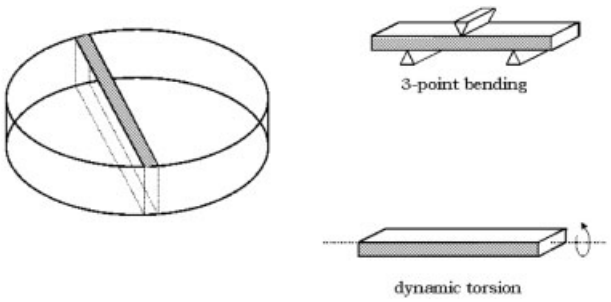

Figure 2 Schematic of sample machining from the sintered pieces for mechanical testing.

sample strips were 35 mm long, 2 mm wide, and 1 mm thick. The temperature range (−150°C/+200°C) was scanned at a heating rate of 1°C/min. The storage and loss moduli were computed from integration of the stress and strain functions.

Scanning electron microscopy (SEM) observations of the raw powders were performed on a JEOL 804 microscope operated at an acceleration tension of 22 kV. The fracture surfaces of sintered samples, broken after three-point bending tests, were also analyzed by SEM. The specimens were gold-coated prior to examination.

PHYSICAL CHARACTERIZATION OF THE MATERIALS

In addition to the characteristic data of Table I, several physical data on the materials are worth to be known for optimizing the sintering process.

The SEM micrographs of Figure 3 show the particle morphology of the POM-N, POM-G, and KEP-G powders. The native POM-N powder has roughly spherical particles with a peak distribution diameter about 150 μm. In contrast, the ground POM-G powder has facetted and rather elongated particles with an aspect ratio of about 2. The length distribution of the POM-G particles has a peak at about 150 μm, with a significant content of fine particles in the range 10–20 μm. The particles of the ground KEP-G powder have an aspect ratio close to 2 and an average length of about 150 μm.

The DSC curves of Figure 4 show the melting behavior of the raw powders and compression-molded materials. The onset of melting occurs at about 170 and 165°C for the POM-N and POM-G, respectively [Fig. 4(a)]. The POM-G powder displays a melting behavior very close to that of the compression-molded counterpart: the melting curve shape, melting onset, melting peak, and crystallinity are similar (see Table I). This means that the grinding operation does not significantly affect the crystalline microstructure. The crystal content is preserved, in contrast to previous findings on several semicrystalline polymers.[21] In parallel, the DSC melting curves of the KEP materials [Fig. 4(b)] as well as the thermal data of Table I show that the overall melting curve of KEP-G is very similar to that of KEP-CM, with a melting onset of about 160°C. These data give indication of the maximum temperature to which every material can be heated up without significant melting, during the sintering process.

The loss shear modulus versus temperature, as measured from DMA on the compression-molded materials, is reported in Figure 5. Both POM-CM and KEP-CM exhibit two main relaxation peaks at about −60°C and +120°C, as already reported in literature.[22] The lower temperature relaxation is associated with the glass transition (T_g) of the amorphous phase in the materials. The higher temperature relaxation corresponds to the mechanical relaxation of the crystalline phase ($T\alpha_c$) that arises from the activation of molecular motions in the crystallites. This latter relaxation is

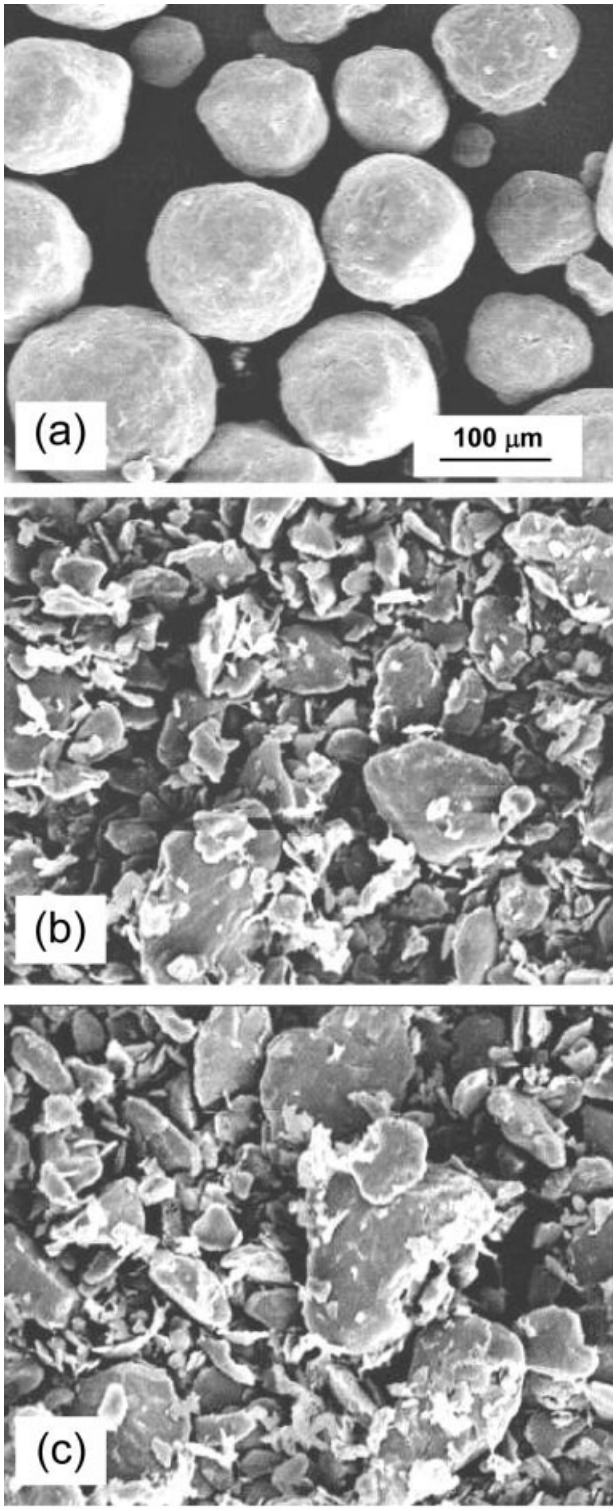

Figure 3 SEM micrographs of the various powders: (a) POM-N native powder, (b) POM-G ground powder, and (c) KEP-G ground powder.

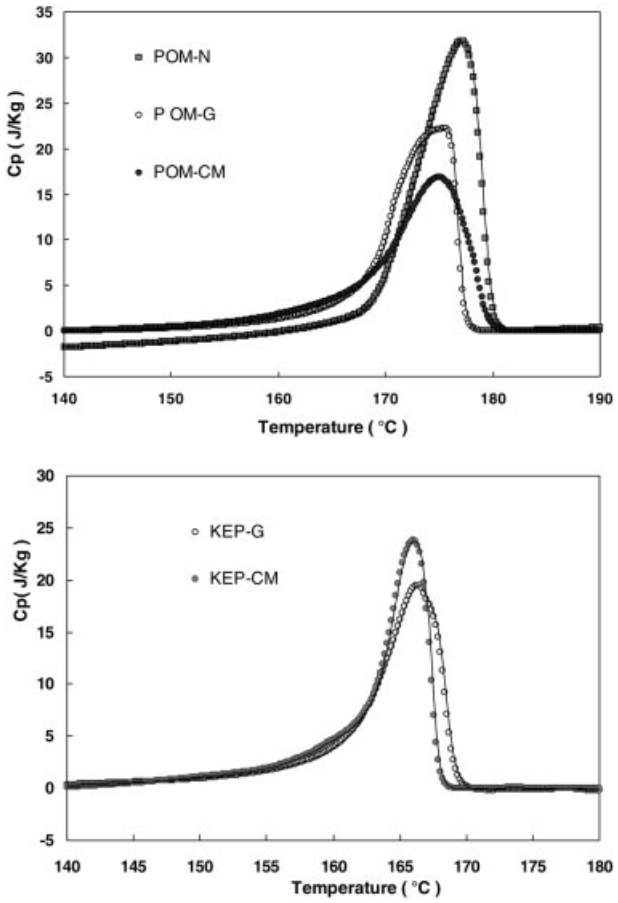

Figure 4 DSC melting curves of (a) the POM-based materials and (b) the KEP-based materials.

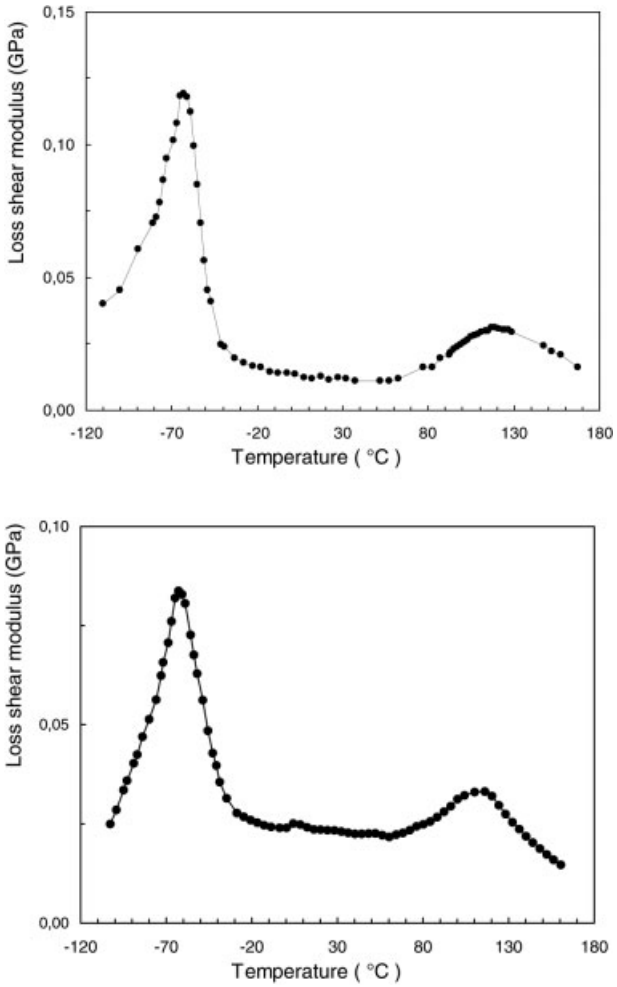

Figure 5 Loss shear modulus versus temperature for (a) the POM-CM and (b) the KEP-CM materials.

peculiarly relevant for the sintering process, since it determines the threshold for molecular diffusion between grains in close contact.

A determining factor for sintering is the plastic flow of the grains under pressure that allows both optimum powder compactness and intimate contact between the grains. Figure 6 displays the evolution with temperature of the compressive yield stress of an injection-molded polyoxymethylene, as reported by Deneuville.[23] The data show that, above 120°C, a compressive stress of about 25 MPa will be enough to impart a plastic deformation on the POM particles during compaction. This is assumed to hold true for the Kepital copolymer due to its lower crystallinity.

SINTERING PROCESS

Temperature adjustment

Sintering of POM in the solid state is used to avoid the drawbacks of melt processing. Therefore, the higher temperature of the process should be the onset of the melting peak that is about 170°C, as judged from the DSC melting curve of Figure 4 for both the POM-N

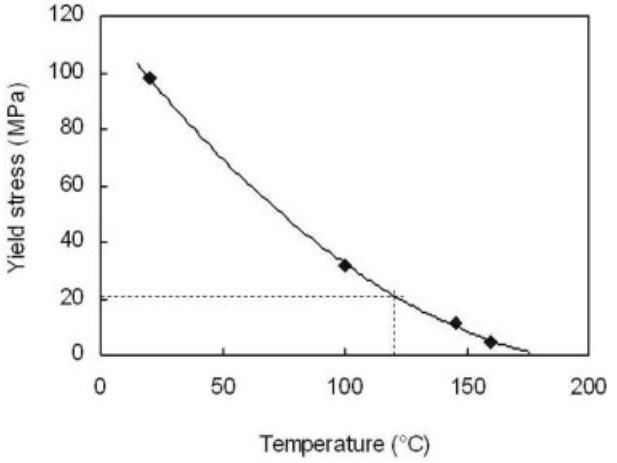

Figure 6 Compressive yield stress versus temperature of injection-molded POM after Ref. 20 (strain rate = 5×10^{-4} s^{-1}; aspect ratio = 1.5).

and POM-G powders. The corresponding temperature will be 160°C for KEP-G.

Regarding the lower temperature limit for the experiment, it is obvious that an active molecular mobility is necessary for the welding of the powder grains, in addition to the plastic shear. Previous studies concerned with glassy polymers, or partially crystalline polymers with high T_g, are somewhat puzzling.[24–26] Compaction experiments have been achieved in a wide range of temperature, from just above T_g to far below T_g. Compaction at RT, i.e., far below T_g, can lead to dense and coherent pieces due to the plastic deformation that allows interlocking of the particles. However, a long pressure-less sintering below T_g brings about better welding of the particles. The pressure-less sintering, close to or above T_g, of powders compacted far below T_g involves a marked recovery of plastic strains accompanied with a loss of density. To sum up, it seems that the temperature domain about T_g is the one leading to the more efficient welding of the powder particles and the best mechanical properties of the compacts, irrespective of pressure-less sintering is carried out or not after compaction.

In the case of semicrystalline polymers, such as polyoxymethylene, that have a glass transition far below RT, the rubbery amorphous phase alone is not liable to provide an efficient sintering effect at RT. Besides, it is quite obvious that very poor sintering effect can be expected for processing temperature below the crystalline relaxation, $Ts\alpha_c$, which determines the activation of molecular mobility in the crystal. Indeed, strong bonding of the crystallites from neighbor powder grains through the grain interface is necessary to provide an efficient transfer of strains and stresses. Therefore, 120°C is certainly the minimum temperature that is likely to enable interchain diffusion and welding of the grains via the crystalline phase.

The most appropriate temperature range for sintering POM-N powders should be thus 120–170°C. Actually, multiple trials of sintering revealed that it is necessary to reach the first stage of melting of the material to achieve the welding of the powder grains. As a matter of fact, sintering below 165°C always led to very brittle pieces, indicating very weak welding of the powder particles. This finding is quite consistent with the conclusion of Ward and Hine regarding the hot compaction of melt-spun UHMWPE fibers into bulk parts.[13] These authors showed that partial melting of the fiber outer sheath leads to a strong bonding of the fibers, and allows keeping intact the fiber core properties, notably the stiffness. In the present case, the temperature adjustment was very acute, and (170 ± 2)°C turned out to be a good compromise for the welding of the powder grains and retaining the high crystallinity of the native powder. Sintering at 175°C resulted in an almost completely molten material with crystallinity and mechanical properties very close to that of the compression-molded material.

Pressure adjustment

The pressure adjustment was made according to the yield stress dependency of POM in compressive test, as reported in Figure 6. A pressure of 25 MPa, i.e., a value above the compressive yield stress at 120°C, proved to be sufficient enough for the compaction of the powders to the theoretical density of the compact material at sintering temperature of 172°C. Endeavors for compacting at higher pressure levels, up to 75 MPa, did not improve the mechanical behavior of the sintered pieces. It is suspected that reduced mobility in the crystalline phase under pressure is responsible for a loss of welding ability of the powder particles. Semicrystalline polymers are indeed highly pressure-sensitive regarding the temperature of phase transitions as well as glass transition.[19] Considering the pressure sensitivity coefficient of 0.16°/MPa for polyoxymethylene,[19] a pressure increase of 50 MPa will shift its melting point by about +8°.

In addition, to the above drawback of a high pressure on the sintering efficiency of POM and KEP, numerous cracks appeared in the samples after unloading, for sintering pressures above 25 MPa. It is suspected that bulk compression rather than plastic shear occurs at high pressure, and that the relaxation upon unloading of elastic stress concentrations about the grains is responsible for the generation of cracks.

Sintering procedure

The sintering cycle is depicted on the temperature and pressure plots versus time of Figure 7. The sample is first heated to the optimum temperature (i.e., 170°C in the case of POM-N) for 15 min without pressure. Then a pressure of about one third the maximum pressure level is applied for 15 min, before applying the maximum pressure of 25 MPa for an additional 15 min. The sample is subsequently unloaded monotonically over a time interval of about 5 min, and allowed to cool down slowly to RT in the compaction cell without pressure.

DENSITY AND CRYSTAL CONTENT

Density measurements are usually carried out for evaluating the compactness of sintered materials. This approach assumes that the bulk density of the granular materials does change during sintering. However, regarding semicrystalline polymers, the crystallinity and therefore the density are well known to depend on thermal treatment. In the case of POM-NS, the apparent density $\rho = 1.45\ g/cm^3$ gives a crystal weight

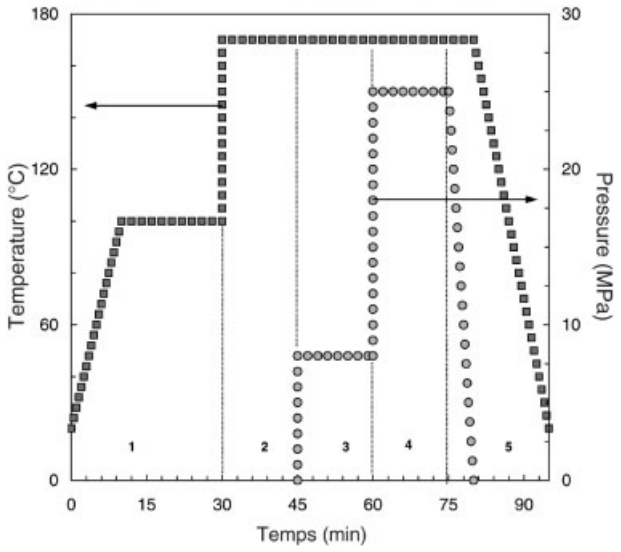

Figure 7 Temperature and pressure profiles versus time for the optimized sintering cycle of the POM-N powder. Stage 1, conditioning at 100°C; Stage 2, preheating at the sintering temperature; Stage 3, application of pressure one-third the maximum value; Stage 4, application of full pressure; and Stage 5, slow unloading and slow cooling.

fraction of 88%, which is amazingly close to that obtained from DSC, i.e. 92% (Table I). Considering the uncertainties on the melting enthalpy of perfectly crystalline polyoxymethylene as well as on the crystal and amorphous phase densities, this finding gives evidence that POM-NS has both very high crystallinity and extremely low porosity, if any.

Table I also reveals a significant crystallinity increase of all the sintered materials with respect to the corresponding powders: the figures are about +6% for POM-NS, +18% for POM-GS, and +13% for KEP-GS. This finding suggests a high molecular mobility in the crystalline phase at the sintering temperature, which allows both the welding of the particles via the crystallites close to the surface, and a partial crystallization of the amorphous chain segments; thanks to the short-range reorganization in the crystalline phase. The striking increase of melting point of POM-NS, as compared to the native powder, is relevant to a crystal size increase, which corroborates a high level of crystal reorganization due to the molecular mobility in the crystalline phase during sintering. The mechanism of crystal perfection will be discussed in a following paper.[27]

MECHANICAL BEHAVIOR

Three-point bending

Flexure tests have been carried out on POM-based and KEP-based materials. The equivalent tensile stress–strain data are reported in Figure 8. Compression-molded samples, POM-C and KEP-CM, are highly ductile and do not break in this kind of experiment. In contrast, sintered materials always break at low strain, although they are not actually brittle. A piece of evidence of the nonbrittleness of the sintered pieces is their very good ability for machining, more precisely cutter-milling and drilling.

Noteworthy is the improved stiffness of the sintered materials with respect to the CM ones, as judged from the slope of the stress–strain curves, which gives the modulus of the material (Fig. 8). Table II reports the tensile modulus data for the various sintered and compression-molded samples. A remarkable twofold increase is observed for POM-NS as compared with POM-CM. This is a direct consequence of the significant increase of crystallinity during the sintering treatment. However, further discussion about the stiffness increase is made later taking into account the morphological changes.

Regarding the POM-based materials, POM-GS is more ductile and less stiff than POM-NS. It seems that the particle welding during sintering has been more

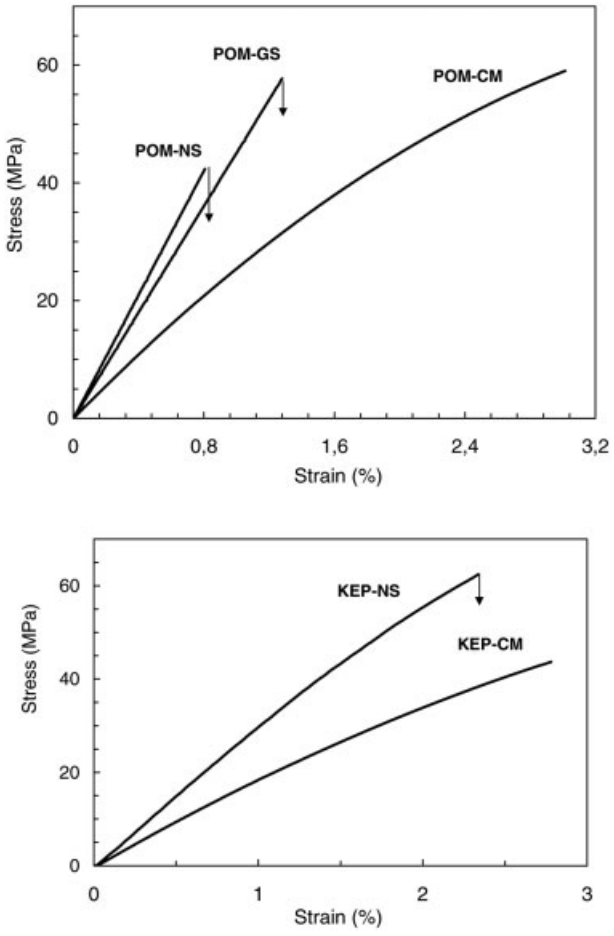

Figure 8 Equivalent stress–strain curves derived from three-point bending tests on (a) the POM-based and (b) the KEP-based materials.

TABLE II
Modulus Data for the Sintered and Compression-Molded Materials

Material	Young's modulus (GPa)	Shear modulus (GPa)
POM-NS	5.3 ± 0.2	2.3 ± 0.1
POM-GS	4.5 ± 0.2	1.8 ± 0.1
POM-CM	2.8 ± 0.1	1.3 ± 0.1
KEP-GS	3.0 ± 0.2	1.2 ± 0.1
KEP-CM	1.9 ± 0.1	0.8 ± 0.1

effective for PM-GS. The reason may be that the lower crystallinity of the POM-G powder allows easier plastic flow of the particles and better shear-induced contact of the particle-interfaces. In contrast, the lower stiffness of POM-GS is relevant to a lower increase of crystallinity during sintering that is corroborated by the data of Table I. It is, however, worth noticing that the relative increase of crystallinity is much greater for POM-GS than that for POM-NS. This is due to the lower crystal content of the ground powder that affords a greater capability of molecular reorganization during sintering, as compared with the native powder.

Compressive tests

Stress–strain curves from compressive tests are reported in Figure 9 for the POM-CM and POM-NS. In the elastic domain, the curves are very similar to the ones from the three-point bending tests, respectively, for the two materials. This means that the Young's modulus is the same for the two kind of tests, namely about 2.8 GPa for POM-CM and about 5.3 GPa for POM-NS (Table II).

Beyond a strain level of about 2%, POM-CM displays a clear cut departure from linearity that is relevant to the activation of anelastic or viscoelastic processes for a stress level of 60 MPa. Then, POM-CM deforms plastically at a flow stress of about 90 MPa, as determined from the stress plateau beyond 4% strain. In contrast, POM-NS exhibits a steady linear behavior up to rupture at 135 MPa. At this stress level, the bulk samples suddenly break as a whole and collapse into grains about a few hundreds of micrometers. These grains consist of only a few elementary powder particles. This observation suggests that the sintering-induced welding concerns a very thin material layer at the surface of the contacting particles. Notwithstanding, the 135 MPa value for the breaking stress of POM-NS, which largely exceeds the plastic flow stress of POM-CM, is relevant to an efficient welding of the powder particles. Besides, this finding suggests that the POM-NS crystalline phase is intrinsically unable to activate plastic processes as a result of the structural reorganization due to sintering, namely the crystal perfection improvement and the crystallinity increase.

Dynamic mechanical behavior

The shear modulus data from DMA are reported in Figure 10 for POM-based and KEP-based materials. Below the lower temperature relaxation, the modulus is little sensitive to the processing method, for both homopolymer and copolymer. The stiffness ranking roughly follows that of the crystallinity index, which means that the crystal modulus is somewhat higher than that of the amorphous phase in the glassy state. The trend is similar to that reported by Boyd[28] in the case of annealed high density polyethylene crystallized from the melt, for equivalent crystal contents. In the whole temperature domain between the glass transition and the crystalline relaxation, the three POM-based materials display a striking modulus increase in the order POM-CM < POM-GS < POM-NS. As already pointed out in the case of the tensile modulus, this ranking of the POM-based materials parallels the crystallinity increase. The same observation holds for the copolymer, the KEP-GS being stiffer and more crystalline than the KEP-CM.

The stiffness increase of the sintered materials, as compared with compression-molded parents, is surprisingly greater than the corresponding increase in crystallinity. For a more acute analysis, the RT shear modulus data of the three POM-based materials are reported in Figure 11 as a function of the crystal volume fraction. Figure 11 also displays the predicted shear modulus curves for the Voigt and Reuss models featuring the parallel and series mechanical coupling of the crystalline and the amorphous phase in semicrystalline polymers. The corresponding equations are $G_{(\text{series})} = G_c\phi_c + G_a\,(1 - \phi_c)$ for the series coupling, and $G_{(\text{parallel})} = 1/[(1 - \phi_c)/G_a + \phi_c/G_c]$ for the par-

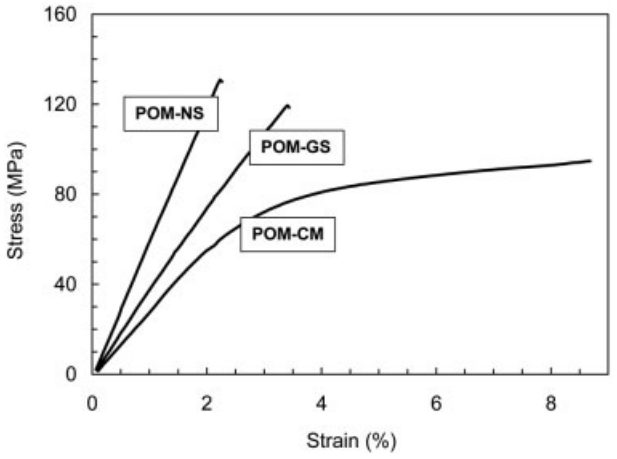

Figure 9 Stress–strain curves under compressive testing of the POM-based materials.

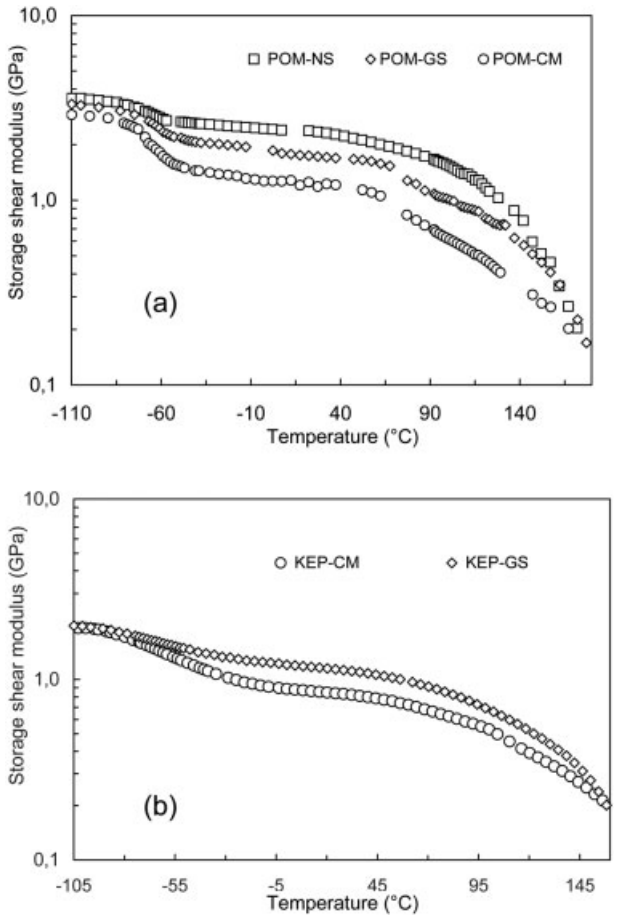

Figure 10 Storage shear modulus versus temperature for (a) the POM-based and (b) the KEP-based materials.

allel coupling, assuming G_c = 3.5 GPa and G_a = 0.1 GPa for the crystal and amorphous moduli of POM at RT. The parallel coupling is the upper bound for heterogeneous materials modulus: it is relevant to a continuous or percolating structure of the stiff component, i.e., the crystalline phase in the present case. The series coupling is the modulus lower bound: it is relevant to a high degree of dispersion of the stiff component. The proximity to the parallel model is more particularly indicative of a great connectivity of the crystalline phase throughout the material. The experimental data of Figure 11, for the three POM-based materials, reveal an increasing degree of parallel coupling of 50, 55, and 67% for the POM-CM, POM-GS, and POM-NS, respectively. Therefore, it can be concluded that crystal percolation or connectivity increases in the order POM-CM < POM-SG < POM-SN. This is indirect evidence, nevertheless a strong hint, that sintering proceeds via an actual welding of the crystallites across the interface between neighbor powder particles.

The theoretical RT crystal modulus, G_c = 3.5 GPa, which determines the upper limiting modulus of the two models, is taken from the higher modulus value of the experimental data of Figure 10 at low temperature. This choice is based on the assumptions that the modulus of the amorphous component below T_g is not far from that of the crystal, and that G_c depends very little on temperature between T_g and RT. Notwithstanding, if the above assumptions were not rigorously obeyed, it is worth noticing that taking a ±20% different value for G_c would lead to the same earlier conclusion. Regarding the RT theoretical modulus of the rubbery amorphous component, which holds for the lower limiting modulus of the two models, the value G_a = 0.1 GPa has been borrowed from data for the isotropic amorphous phase of flexible-chain semicrystalline polymers such as polyethylene.[29] This G_a value is consistent with that of highly entangled or crosslinked rubbers.[30] In the eventuality that this figure was erroneous, a lower G_a value would have negligible incidence on the previous conclusion due to the very high gap between the upper and lower modulus limits of the model.

The comparison of the homopolymer and copolymer stiffness data also deserves some comment. In spite of lower crystallinity (Table I), the sintered copolymer KEP-GS is as stiff as the compression-molded homopolymer POM-CM (see Table II). This is an additional piece of evidence that sintering involves a structural modification, which results in a greater connectivity of the crystalline phase. A better mechanical coupling of the crystallites in KEP-GS, i.e., a greater proportion of parallel coupling as compared with POM-CM, provides a compensation for its lower crystal content.

MORPHOLOGY OF FAILURE SURFACES

In contrast to the sample collapse under compressive test, brittle rupture under three-point bending of the

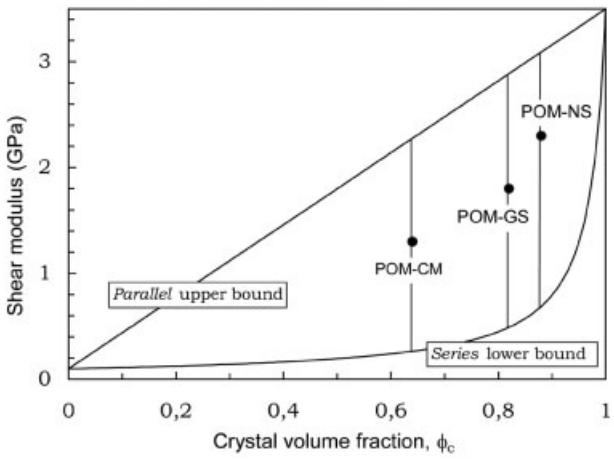

Figure 11 Predicted storage shear modulus of semicrystalline polymers versus crystal volume fraction for the two limiting parallel and series models; the individual data reported on the graph are featuring the three POM-based bulk samples.

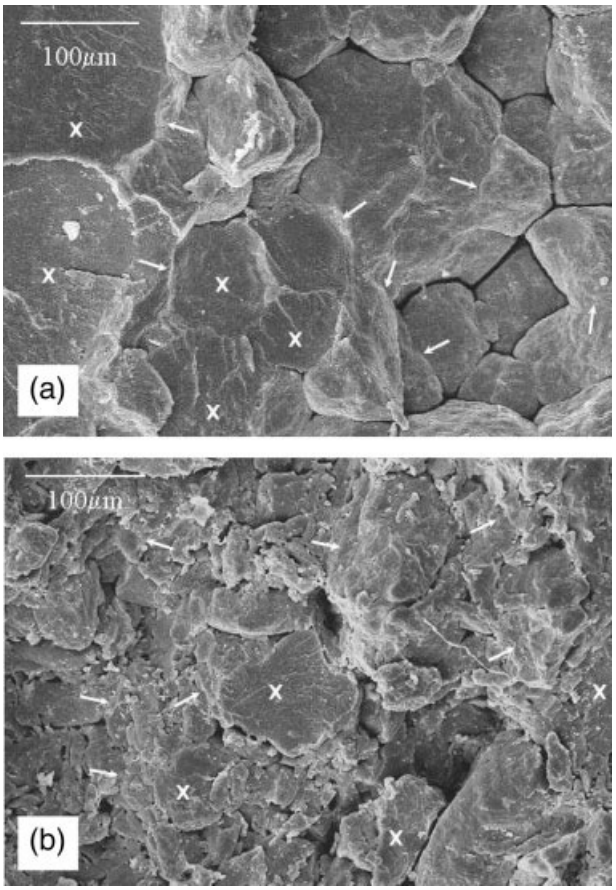

Figure 12 SEM micrographs of fracture surfaces of (a) POM-NS and (b) POM-GS samples after three-point bending rupture (the arrows indicate the locus of strong interparticle bonding; the × symbols indicate the trans-particle failure).

sintered materials results from the propagation of a single crack normal to the sample surface. This enables direct visualization of the rupture process. The SEM micrographs of Figure 12 show the fracture surfaces of POM-GS and POM-NS samples, following a three-point bending test up to rupture. Predominent intergranular failure is observed for both materials. However, strong intergranular bonding is clearly observable at several loci of the micrographs. This is a piece of evidence of the efficient welding of the powder grains via local diffusion. A more detailed analysis of the welding mechanisms is reported in a companion paper.[27]

It is worth noticing that trans-granular failure events are also clearly observable for both POM-NS and POM-GS. This finding provides additional support to the efficiency of the grain welding, together with an evidence of the great brittleness of the grains after the sintering process. This is consistent with the compressive behavior of the materials, which revealed a high strength without any signs plasticity of the sintered samples, notably in the case of the POM-NS material.

CONCLUDING DISCUSSION

The sintering efficiency of POM and Kepital powders is highly sensitive to temperature in the vicinity of the melting temperature domain. Some very local melting of the low melting temperature crystals seemed to be necessary for an efficient welding of the powder particles via surface welding. However, most of the native crystalline phase should be preserved from melting for preventing a crystallinity drop.

A nearly twofold increase of modulus is observed between compression-molded and the sintered native powder for the homopolymer. This stiffness improvement is shown to be significantly greater than the sole effect of the crystallinity increase: it is concluded that the sintered material display a greater continuity of the stiff crystalline phase as compared with the compression-molded one. This is a piece of evidence of particle welding owing to the compression-induced shear of the particles in combination with the molecular diffusion in the crystalline phase and at the interface between neighboring crystallites.

It is worth noticing that intermeshing of chain segments in the amorphous phase may also possibly occur at the particle interface owing to the partial melting of the more defective crystallites, in conjunction with the compression-induced shear of the powder particles.

The compressive behavior of the sintered materials reveals a very high stiffness of the crystalline phase, without any plastic capabilities, which contrasts with the pieces compression-molded from the melt. This thoroughly supports the hypothesis of a high level of crystal continuity.

A companion paper[27] is dealing with the structural characterization of the morphological changes following sintering to elucidate the mechanisms of particle welding. This paper supports a solid state welding model for sintering, with minor contribution from melting. Demonstration is made of a spectacular crystalline reorganization via molecular diffusion during sintering, as judged from the large shift to higher temperature of both the crystalline relaxation and the melting peak. Small-angle X-ray scattering reinforces the evidence of large scale crystalline reorganization during sintering, together with ordering of the folding surface.

References

1. Narkis, M. In Polymer Powder Technology; Narkis, M.; Rosenzweig, N., Eds.; Wiley: New York, 1995; Chapter 10.
2. Jog, P. J. Adv Polym Technol 1993, 12, 281.
3. Ariawan, A. B.; Ebnesajjad, S.; Hatzikiriakos, S. G. Powder Technol 2001, 121, 249.
4. Han, K. S.; Wallace, J. F.; Truss, R. W.; Geil, P. H. J Macromol Sci B: Phys 1981, 19, 313.
5. Zachariades, A. E. Polym Eng Sci 1985, 25, 747.

6. Statton, O. W. J Appl Phys 1967, 38, 4149.
7. Rastogi, S.; Kurelec, L.; Cuijpers, J.; Lippits, D.; Wimmer, M.; Lemstra, P. J. Macromol Mater Eng 2003, 288, 964.
8. Rein, D. M.; Shavit, L.; Khalfin, R. L.; Cohen, Y.; Terry, A.; Rastogi, S. J Polym Sci Part B: Polym Phys 2004, 42, 53.
9. Kanamoto, T.; Sherman, E. S.; Porter, R. S. Polym J 1979, 11, 497.
10. Rotzinger, B. P.; Chanzy, H. D.; Smith, P. Polymer 1989, 30, 1814.
11. Pawlikowski, G. T.; Mitchell, D. J.; Porter, R. S. J Polym Sci Part B: Polym Phys 1988, 26, 1865.
12. Porter, R. S.; Kanamoto, T.; Zachariades, A. E. Polymer 1994, 35, 4979.
13. Ward, I. M.; Hine, P. J. Polym Eng Sci 1997, 37, 1809.
14. Yan, R. J.; Hine, P. J.; Ward, I. M.; Olley, R. H.; Bassett, D. C. J Mater Sci 1997, 32, 4821.
15. Morye, S. S.; Hine, P. J.; Duckett, R. A.; Carr, D. J.; Ward, I. M. Compos A: Appl Sci Manuf 1999, 30, 649.
16. Jordan, N. D.; Olley, R. H.; Basset, D. C.; Hine, P. J.; Ward, I. M. Polymer 2002, 43, 3397.
17. Ward, I. M.; Hine, P. J. Polymer 2004, 45, 1413.
18. Dolce, T. J.; Grates, J. A. In Encyclopedia of Polymer Science and Engineering; Mark, H. F., Bikales, N. M., Overberger, C. G.; Menges, G., Eds.; Wiley Interscience: New York, 1985; Vol. 1, p 42.
19. Wunderlich, B. Macromolecular Physics, Vol. 3: Crystal Melting; Academic Press: New York, 1980; Chapter 8.
20. Wunderlich, B. Macromolecular Physics, Vol. 1: Crystal Structure, Morphology, Defects; Academic Press: New York, 1980; Chapter 4.
21. Lovinger, A. J.; Belfiore, L. A.; Bowner, T. N. J Polym Sci Part B: Polym Phys 1985, 23, 1449.
22. McCrum, N. G.; Read, B. E.; Williams, G. Anelastic and Dielectric Effects in Polymer Solids; Dover: New York, 1967; Chapter 14.
23. Deneuville, P. Ph.D. Thesis, Centre de Mise en Forme des Matériaux, Ecole des Mines de Paris, Sophia Antipolis, France, 1982.
24. Throne, J. L. Adv Polym Technol 1989, 9, 281.
25. Reilly, J. J.; Kamel, I. L. Polym Eng Sci 1989, 29, 1456.
26. Vick, L. W.; Kander, R. G. Polym Eng Sci 1998, 38, 1824.
27. Al Jebawi, K.; Sixou, B.; Vigier, G.; Seguela R. J Appl Polym Sci, to appear.
28. Boyd, R. H. Polymer 1985, 26, 323.
29. Holliday, L. Structure and Properties of Oriented Polymers; Ward, I. M., Ed.; Applied Science: London, 1975.
30. Nielsen, L. E. Mechanical Properties of Polymers and Composites; Marcel Dekker: New York, 1974.